iScience

CellPress

Article

High-Resolution Plasma Membrane-Selective Imaging by Second Harmonic Generation

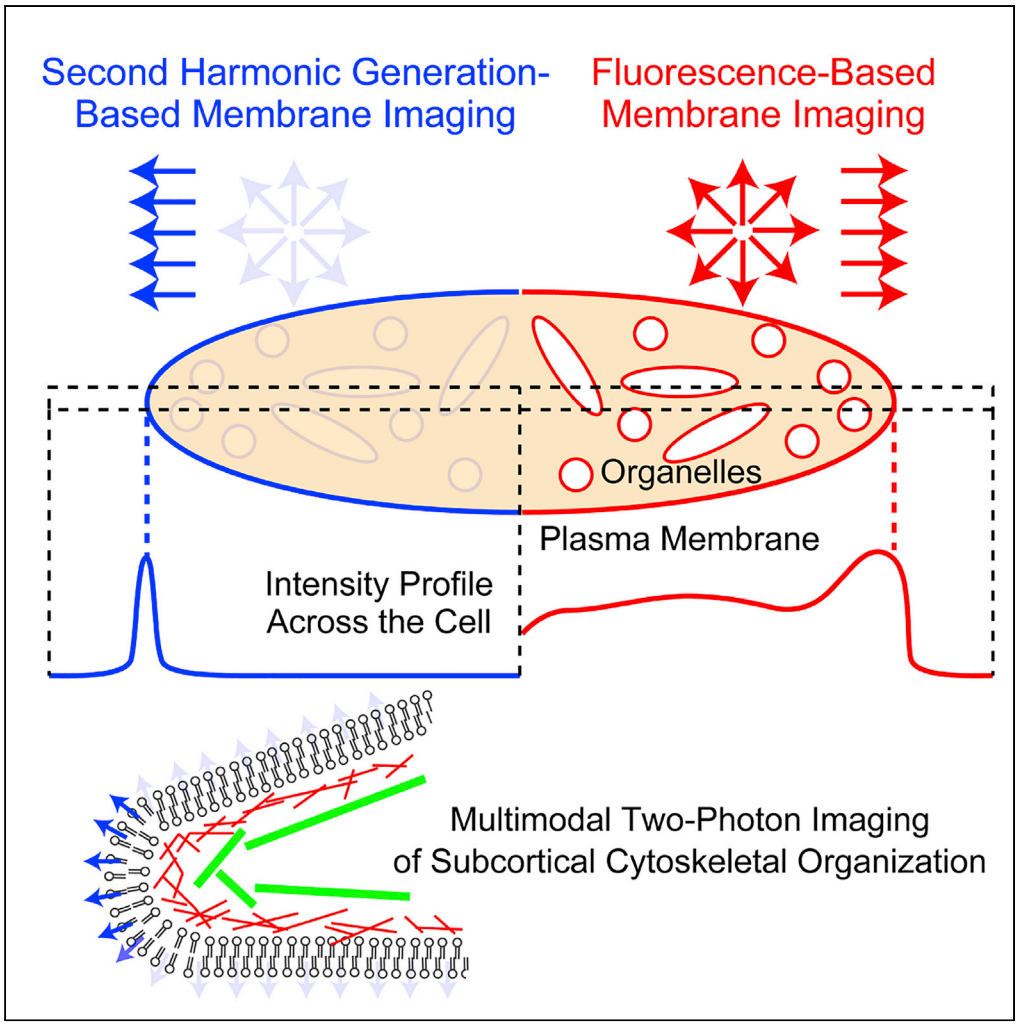

Takaha Mizuguchi, Masato Yasui, Mutsuo Nuriya

mnuriya@z2.keio.jp

HIGHLIGHTS

Dye-based SHG imaging can specifically visualize the plasma membrane

SHG imaging can identify the location of the plasma membrane with high precision

Multimodal imaging reveals the precise organization of subcortical cytoskeletons

Mizuguchi et al., iScience 9, 359–366
November 30, 2018
https://doi.org/10.1016/j.isci.2018.11.008

iScience

CellPress

Article

High-Resolution Plasma Membrane-Selective Imaging by Second Harmonic Generation

Takaha Mizuguchi,[1] Masato Yasui,[1] and Mutsuo Nuriya[1,2,3,4,*]

SUMMARY

The plasma membrane is the site of intercellular communication and subsequent intracellular signal transduction. The specific visualization of the plasma membrane in living cells, however, is difficult using fluorescence-based techniques owing to the high background signals from intracellular organelles. In this study, we show that second harmonic generation (SHG) is a high-resolution plasma membrane-selective imaging technique that enables multifaceted investigations of the plasma membrane. In contrast to fluorescence imaging, SHG specifically visualizes the plasma membrane at locations that are not attached to artificial substrates and allows high-resolution imaging because of its subresolution nature. These properties were exploited to measure the distances from the plasma membrane to subcortical actin and tubulin fibers, revealing the precise cytoskeletal organization beneath the plasma membrane. Thus, SHG imaging enables the specific visualization of phenomena at the plasma membrane with unprecedented precision and versatility and should facilitate cell biology research focused on the plasma membrane.

INTRODUCTION

The plasma membrane serves as a platform for cell-to-cell communication and intracellular signal transduction, and thus, its selective imaging is critical for cell biology research (Grecco et al., 2011; Steyer and Almers, 2001). Currently, however, it is difficult to detect the precise location of the plasma membrane in living cells. Membrane-anchored fluorescent proteins and membrane-selective organic fluorescent dyes are widely used for this purpose, but the dynamic trafficking of membrane structures within living cells produces signals arising not only from the plasma membrane but also from various intracellular membrane structures, such as the ER and endocytosis/exocytosis vesicles. Fluorescence signals from these intracellular membrane structures results in background noise in the visualization of the plasma membrane, making its precise identification impossible. For example, docked synaptic vesicles reside beneath the plasma membrane, at a distance of less than 100 nm, which is far below the optical resolution of conventional microscopy. Even recent advancements in super-resolution microscopy cannot resolve this issue (Shim et al., 2012). In addition, chromatic aberrations cannot be completely eliminated when using different excitation wavelengths, making spatial comparisons difficult, even for two-colored signals. To overcome these limitations for the characterization of the plasma membrane, a non-fluorescence-based approach is necessary.

In sharp contrast to fluorescence-based imaging, second harmonic generation (SHG) requires materials lacking centrosymmetry. The stringent requirement with respect to molecular orientation provides SHG imaging with a special capacity to visualize molecular orientation-sensitive phenomena within cells and tissues (Pavone and Campagnola, 2013). For example, well-ordered collagen fibers serve as a good SHG source in tissues and therefore can be visualized without staining, which has diagnostic applications for discriminating between the collagen fiber organizations of healthy and tumor tissues (Brown et al., 2003). Such orientation-selective molecular imaging can be further exploited by visualizing specific exogenous molecules that do not show a centrosymmetric distribution within cells. The most prominent and abundant asymmetric sites in cells reside in membrane structures, where the water-rich hydrophilic environment is apposed to the lipid-rich hydrophobic lipid-bilayer. In fact, many organic fluorescent dyes designed to visualize membrane structures generate SH (second harmonic) signals from biological membranes when illuminated with ultra short-pulse lasers (Reeve et al., 2010), and these have been utilized to investigate the biophysical properties of membranes (Ben-Oren et al., 1996; Campagnola et al., 1999). Although SHG imaging is a powerful technique, the use of fluorescent dyes for this purpose makes it difficult to simultaneously image it with other fluorescent markers, limiting its uses in cell biology, where multifaceted analyses are often required. To overcome this issue, we have recently developed a non-fluorescent SHG-specific dye, Ap3 (Nuriya et al., 2016). When combined with other fluorescent probes, this dye

[1]Department of Pharmacology School of Medicine, Keio University, 35 Shinanomachi, Shinjuku, Tokyo 160-8582, Japan

[2]Graduate School of Environment and Information Sciences, Yokohama National University, Kanagawa 240-8501, Japan

[3]Precursory Research for Embryonic Science and Technology (PRESTO), Japan Science and Technology Agency (JST), Kawaguchi, Saitama 332-0012, Japan

[4]Lead Contact

*Correspondence: mnuriya@z2.keio.jp

https://doi.org/10.1016/j.isci.2018.11.008

can be utilized for multimodal two-photon imaging to obtain SHG-based and two-photon fluorescence (TPF)-based signals without any signal contamination or interference; this approach has extensive potential applications for plasma membrane research. However, verification of the specificity and accuracy of signals at the plasma membrane is necessary for applications to cell biology research.

In this study, we characterized dye-based SHG imaging of the plasma membrane and explored the potential use of multimodal two-photon imaging to investigate the cell biology of plasma membranes that are not attached to artificial substrates. Our results establish SHG imaging as a unique and powerful high-resolution plasma membrane-selective imaging tool that can be readily applied to cell biology research.

RESULTS

Comparison between Plasma Membrane Imaging with Membrane-Anchored GFP-TPF and Ap3-SHG

Membrane-bound GFP and other fluorescent proteins are widely used to visualize cell membrane structures, including the plasma membrane. Therefore, we first compared the plasma membrane images obtained by membrane-bound GFP TPF (Zacharias et al., 2002) and SHG from the amphiphilic non-fluorescent SHG-specific dye Ap3 (Nuriya et al., 2016) using CHO (Chinese Hamster Ovary) cells.

CHO cells plated on poly-L-lysine-coated coverslips were infected with baculovirus containing a gene encoding a membrane-anchored GFP fused to the myristoylation/palmitoylation sequence of Lck tyrosine kinase that targets GFP to the membrane (Celik et al., 2013; Quader et al., 2014; Resh, 1999) and incubated for 2–3 days to allow the expression of the introduced gene. The cells were stained with Ap3 right before imaging and illuminated with a femtosecond laser at 950 nm under a laser scanning microscope. The dye was present throughout the experimental period, ensuring stable SHG images without significant phototoxicity (Nuriya et al., 2016). Importantly, the non-fluorescent and SHG-active property of the SHG-specific dye Ap3 ensures a lack of cross-contamination between signals from SHG and fluorescent probes, allowing completely independent simultaneous signal acquisition (Nuriya et al., 2016). Despite overlap at the plasma membrane, the images based on Ap3-SHG and GFP-TPF exhibited robust differences; a clear line-like signal was detected solely at the plasma membrane for SHG, and more diffuse signals, including strong intracellular signals, were detected from GFP (Figure 1A). The differences between the two images were evident not only at a low magnification that visualizes all cellular structures with various intracellular organelles (Figure 1A) but also at a higher magnification (Figure 1B). When the periphery of the cell was imaged, although the SHG signal exhibited a sharp line at the plasma membrane, GFP signals were more continuous from the plasma membrane to the intracellular regions, as shown in the plot profile (Figures 1B and 1C).

The observed intracellular signals might originate from endocytosed vesicles. This possibility was examined by visualizing membrane-anchored GFP-TPF and Ap3-SHG signals together with endocytosed vesicles loaded with 10-kDa dextran-conjugated Alexa Fluor 594. Indeed, some intracellular membrane-anchored GFP-TPF signals colocalized with endocytosed vesicles (Figure 1D). Further supporting the origin of the membrane-anchored GFP signals, live imaging of these vesicles revealed that the intracellular signals were mobile endocytosed vesicles, whereas the SHG signal was stable throughout the imaging period (Video S1). These results suggest that membrane-bound fluorescent probes are powerful for the visualization of all membrane structures in the cell, including the periphery of the cell, but cannot be utilized to specifically highlight the plasma membrane. In contrast, when cells were stained with the SHG-active amphiphilic dye, SHG imaging was plasma membrane-selective.

Characterization of Ap3-SHG Signals at the Plasma Membrane

The comparison between SHG and TPF signals demonstrated the very narrow and sharp nature of SHG signals at the plasma membrane, which appear to follow a Gaussian distribution based on an analysis of the plot profile (Figure 1C). Therefore, we quantitatively evaluated the validity of Gaussian fitting to the Ap3-SHG signals at the plasma membrane (Figures 2A and 2B). Indeed, the intensity profiles of Ap3-SHG were well fit by a Gaussian curve (Figure 2C, $R^2 = 0.9931 \pm 0.0067$, n = 24).

The width of the plasma membrane is less than 10 nm, which is well below the spatial resolution of the two-photon microscope, and Ap3-SHG signals at the plasma membrane exhibit a Gaussian shape, suggesting that Ap3-SHG at the plasma membrane originated from Ap3 confined to a subresolution region. For

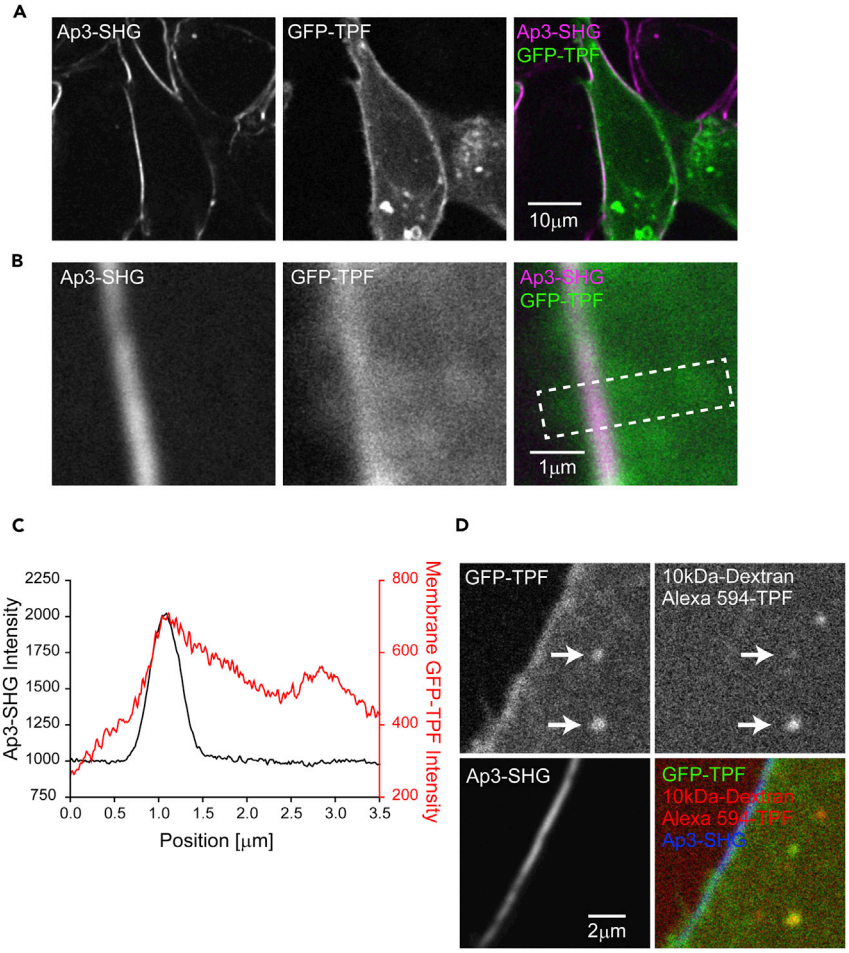

Figure 1. Comparison between Membrane-Anchored GFP-TPF and Ap3-SHG

(A) Representative images of simultaneously visualized membrane-anchored GFP-TPF and Ap3-SHG signals in CHO cells. In the merged image, membrane-anchored GFP-TPF and Ap3-SHG signals are shown in green and magenta, respectively. Scale bar represents 10 μm.

(B) Higher magnification images of the cell shown in (A). Scale bar represents 1 μm.

(C) Plot profile analysis of membrane-anchored GFP-TPF (red) and Ap3-SHG (black) signals in the dotted area shown in (B).

(D) Representative images of endocytosed vesicles labeled by 10 kDa-dextran Alexa Fluor 594 (red), membrane-anchored GFP (green), and Ap3 (blue). Fluorescence signals of membrane-anchored GFP originate not only from the plasma membrane but also from endocytosed vesicles (arrows), but Ap3-SHG is solely detected at the plasma membrane. Scale bar represents 2 μm.

comparison, we analyzed the pattern of TPF signals from fluorescence beads of a subresolution size (spherical beads 100 nm in diameter). We confirmed that the TPF signal from the subresolution beads showed a Gaussian shape, similar to Ap3-SHG at the plasma membrane (R^2 = 0.9931 ± 0.0017, n = 11). The full width at half maximum of the plasma-membrane Ap3-SHG signal was 464 ± 46 nm (n = 24), comparable with that of the TPF signal from 100 nm subresolution beads (525 ± 53 nm, n = 11). Combined with the data in Figure 1, these results demonstrate that SHG imaging can identify the plasma membrane location with a precision and accuracy that was not possible under fluorescence-based imaging. Notably, when cells were imaged at various heights, SHG intensity was the highest where the plasma membrane was perpendicular to the imaging field, but virtually absent where the plasma membrane was parallel (Figure 2D). Taken together, these data suggest that only SHG dyes at the edge of the plasma membrane can interact with incoming electromagnetic fields from the laser and thus effectively generate SH signals (Figure 2E). Importantly, the plasma membrane visualized by SHG is not attached to an artificial substrate, such as glass or plastic at the bottom of the cell, but exists in the physiological context. The fact that Ap3-SHG at the plasma

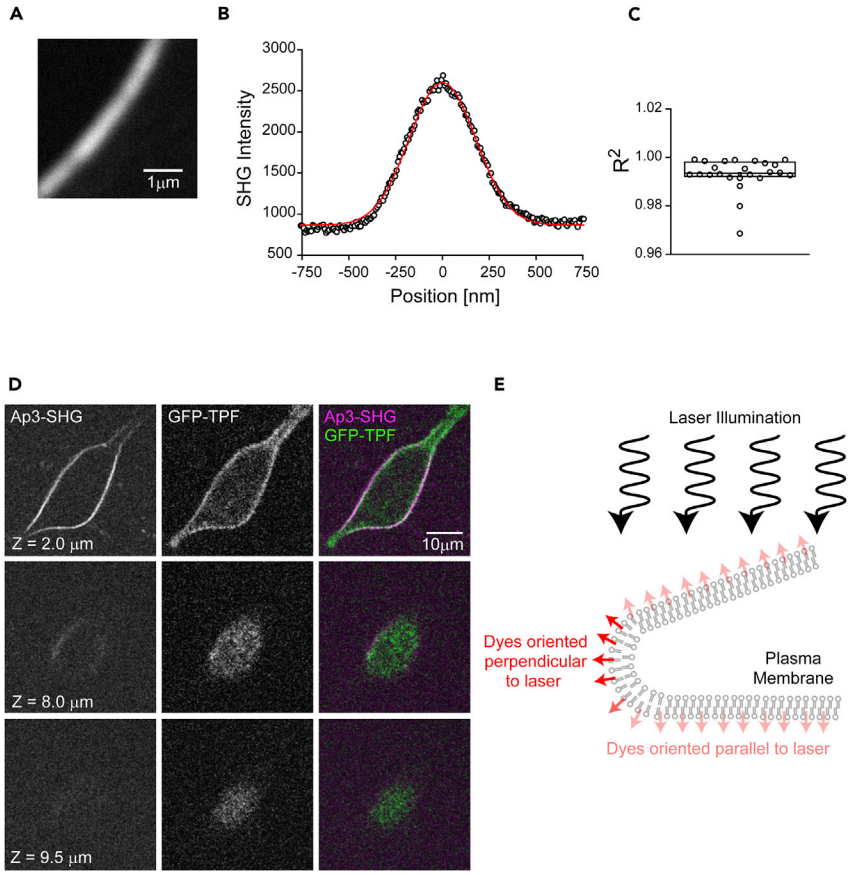

Figure 2. Characterization of Ap3-SHG Signals at the Plasma Membrane

(A) Representative image of the Ap3 SHG signal at the plasma membrane. Scale bar represents 1 μm.

(B) Plot profile of the Ap3-SHG signal shown in (A) across the plasma membrane. The original data (black circles) were fit with a Gaussian function (red line).

(C) Box chart showing the R^2 values for the Gaussian fit of Ap3-SHG signals at the plasma membrane.

(D) Representative images of Ap3-SHG and membrane-anchored GFP-TPF signals at different cell heights. Z-positions indicate the apparent height of the imaging focal plane, measured from the bottom of cells that are attached to the coverslip. Scale bar represents 10 μm.

(E) Schematic illustration showing the site of Ap3-SHG imaging. Ap3 dyes (arrows) are inserted in the plasma membrane, but only those at the edge are aligned perpendicular to the incoming laser generate second harmonic signals.

membrane originates from a point source enables the precise identification of the plasma membrane location according to the peak of the Gaussian fit. These results suggest that SHG plasma membrane analyses allow the determination of the accurate locations of the physiological plasma membrane in living cells.

Characterizations of Peri-Plasma Membrane Cytoskeleton Fibers

Results so far clearly demonstrated that it is difficult to detect the location of the plasma membrane by fluorescent imaging, and this challenge can be resolved by SHG plasma membrane imaging. As a proof of principle, we attempted to determine the precise architectures of subcortical actin and tubulin structures at the physiological plasma membrane. CHO cells were infected with baculoviruses containing genes encoding GFP-tagged actin or tubulin, stained with Ap3, and subjected to imaging. The illumination of these cells allows the visualization of the plasma membrane localization by SHG and subcortical cytoskeleton by GFP-TPF (Figure 3). We then selected locations where actin or tubulin bundle signals were clearly resolved, obtained plot profiles across the plasma membrane, fit plasma membrane SHG and cytoskeletal TPF signals with Gaussian curves, and measured distances between the peaks. These analyses revealed the distributions of actin and tubulin cytoskeleton fibers at the plasma membrane (Figure 4, actin: 257.1 ± 63.2 nm, tubulin: 367.4 ± 28.0 nm, n = 26 for actin, n = 16 for tubulin). A comparison of the two distributions revealed

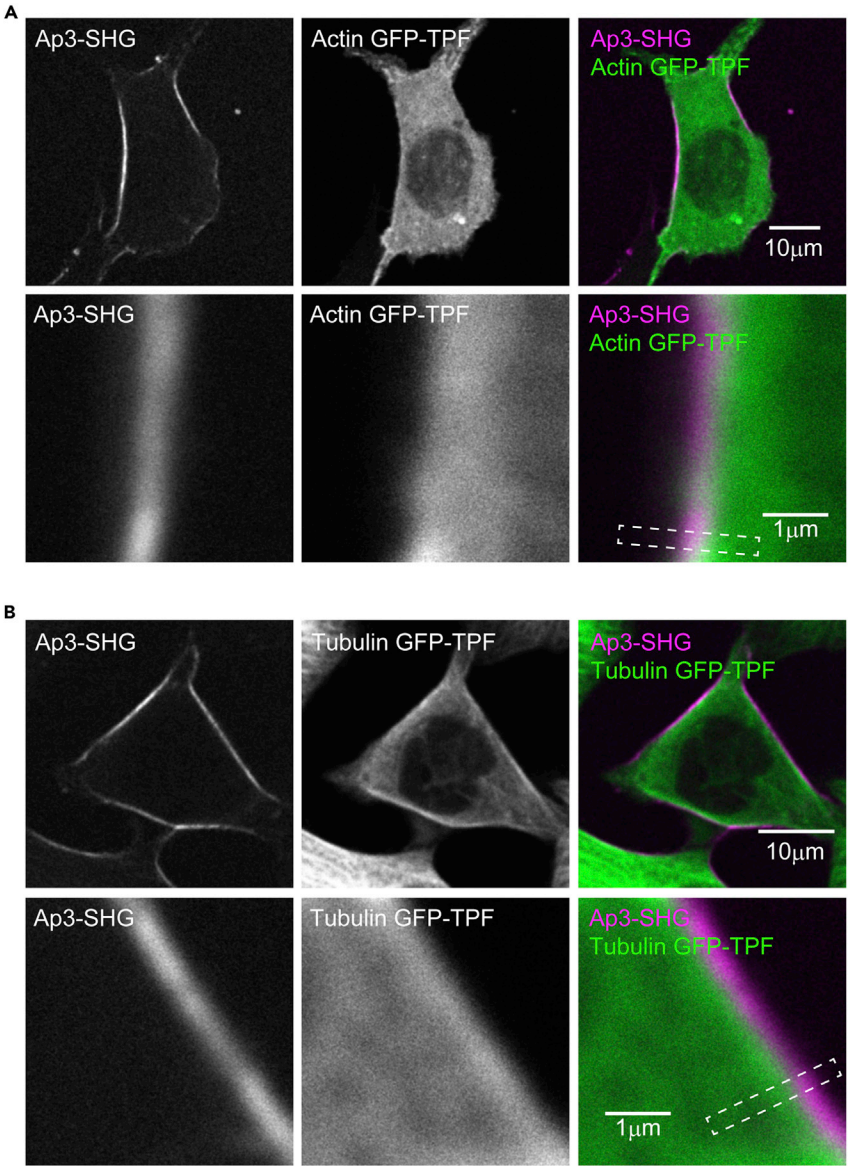

Figure 3. Multimodal Two-Photon Imaging of the Plasma Membrane and Cytoskeleton

(A) Representative images of the plasma membrane and actin visualized by Ap3 and GFP-tagged actin. Scale bars represent 10 μm (top) and 1 μm (bottom), respectively. In the merged image, actin GFP-TPF and Ap3-SHG signals are shown in green and magenta, respectively.

(B) Representative images of the plasma membrane and tubulin visualized by Ap3 and GFP-tagged tubulin. Scale bars represent 10 μm (top) and 1 μm (bottom), respectively. In the merged image, tubulin GFP-TPF and Ap3-SHG signals are shown in green and magenta, respectively.

clear differences between these cytoskeletal structures in terms of their distances from the plasma membrane ($p = 4.0 \times 10^{-6}$, U-test).

DISCUSSION

The identification of the precise location of the plasma membrane is the first step in characterizing biological phenomena at and around the plasma membrane, but conventional fluorescence-based methods are insufficient for this purpose. In this study, we characterized the nature of SHG signals at the plasma membrane and established SHG as a plasma membrane-specific imaging tool. The width of the plasma

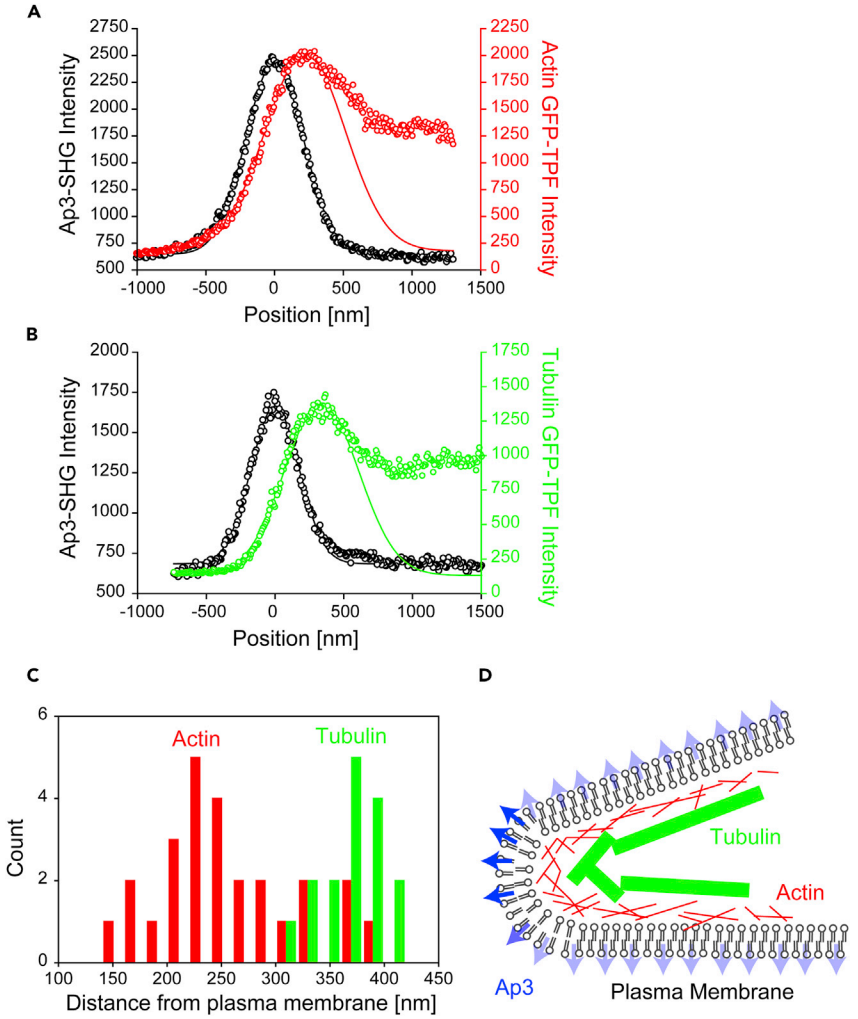

Figure 4. Analyses of Distances from the Plasma Membrane to Intracellular Actin and Tubulin Cytoskeleton

(A) An example of a plot profile showing Ap3-SHG (black) and actin GFP-TPF (red) signal patterns across the plasma membrane corresponding to the region shown in Figure 3A. Open circles show original data, and solid lines show Gaussian fit curves.

(B) An example of plot profiles of Ap3-SHG (black) and tubulin GFP-TPF (green) corresponding to the regions shown in Figure 3B. Open circles show original data, and solid lines show Gaussian fit curves.

(C) Histogram showing the distributions of the distances from the actin and tubulin cytoskeleton to the plasma membrane. The bin size is 20 nm.

(D) Schematic illustration showing the spatial relationship between the plasma membrane and actin and tubulin cytoskeletons.

membrane is less than 10 nm; thus, its precise localization requires the deduction of the origin of a signal derived from an optically unresolvable single point. SHG imaging achieves this since it arises only from the plasma membrane. Importantly, no spectral overlap exists between the SHG signal from the SHG-specific dye and any fluorescent signals generated from the same laser source owing to the Stokes shift of fluorescent signals and the non-fluorescent nature of the SHG-specific dye (Nuriya et al., 2016). This is critical when analyzing two items in close vicinity, such as cortical actin and the plasma membrane, as demonstrated in this study. Furthermore, SHG imaging of the plasma membrane can be used to detect subtle changes in membrane integrity (Moen et al., 2014). SHG is also useful for measuring membrane potentials in neurons (Nuriya et al., 2006; Nuriya and Yasui, 2010; Rama et al., 2010; Sacconi et al., 2006). Taken together, our results establish the plasma membrane selectivity of SHG imaging, which has wide applications in cell biology.

In addition to the fluorescent protein-based approaches examined in this study, small organic fluorescent dyes with affinity to the lipid bilayers have also been applied to visualize the plasma membrane. In particular, a series of amphiphilic fluorescent dyes that are applied extracellularly are readily incorporated to the plasma membrane and emit fluorescence, but these dyes also suffer from rapidly arising intracellular signals owing to dynamic endocytosis/exocytosis. Many of these dyes also generate second harmonic signals at the plasma membrane and thus can be utilized to visualize the plasma membrane (Reeve et al., 2010). However, strong and often broad-spectrum fluorescent signals limit their combined use with other fluorescent reporters with spectral overlap. The SHG-specific non-florescent dye that we recently developed overcomes this limitation and thus enables simultaneous plasma membrane imaging with other reporters (Nuriya et al., 2016). In principle, SHG can also be used to visualize large intracellular organelles where the SHG dye distribution breaks the centrosymmetry. However, we did not observe these structures around the plasma membrane. This can likely be explained by the small diameters of most endocytosed/exocytosed vesicles (<200 nm) (D'Souza-Schorey et al., 1998), which are much smaller than the optical resolution of the conventional two-photon microscopy system; dyes inserted around a vesicle make them centrosymmetric as a whole. The same may be true for larger organelles that are stacked in close proximity.

Total internal reflection fluorescence (TIRF) imaging is another useful imaging method for near-plasma membrane phenomena; it utilizes the limit of evanescent light traveling above the cover glass (Mattheyses et al., 2010). In fact, TIRF imaging has been successfully applied to investigate peri-plasma membrane phenomena, such as exocytosis/endocytosis. However, TIRF visualization is limited to materials that are directly attached to the coverslip. Since the plasma membrane at the bottom of cells attaches to the glass surface via artificial substrates, such as poly-lysine, it may not be representative of physiological conditions. In contrast, SHG visualizes properties at the edge of cells, away from the surface. It should be noted, however, that because SHG imaging is sensitive to orientation, plasma membranes that are parallel to the imaging focal plane cannot be properly visualized. At the same time, optical resolution is higher in the lateral axes than in the axial direction, meaning that the regions visualized through SHG resulted in the most accurate measurement of distances surrounding the plasma membrane. Therefore, the addition of SHG as an imaging tool should contribute to a better understanding of the plasma membrane and nearby structures.

In conclusion, SHG using an amphiphilic SHG-specific dye at the plasma membrane showed a sharp single-point origin signal that can be utilized to identify the location of the plasma membrane with unprecedented precision. Thus, multimodal two-photon imaging with the plasma membrane-specific SHG and fluorescent markers provides a unique and powerful tool for cell biology research.

Limitations of the Study

As mentioned earlier, owing to orientation selectivity, plasma membranes that are parallel to the imaging focal plane cannot be visualized by SHG imaging. Moreover, in densely packed tissues where the plasma membrane of one cell is attached to that of another cell, extracellularly applied SHG dyes will align in the opposite direction at the interface, and therefore, the SHG signal may be canceled; this limitation can be overcome by applying the dye intracellularly.

METHODS

All methods can be found in the accompanying Transparent Methods supplemental file.

SUPPLEMENTAL INFORMATION

Supplemental Information includes Transparent Methods and one video can be found with this article online at https://doi.org/10.1016/j.isci.2018.11.008.

ACKNOWLEDGMENTS

This work was supported by JSPS KAKENHI (16K07065 & ResonanceBio 16H01434) and JST PRESTO (JPMJPR17G6). We would like to thank Olympus Corporation for continuous support in the development of SHG microscopy.

AUTHOR CONTRIBUTIONS

T.M., M.Y., and M.N. designed the research; T.M. and M.N. performed the research and analyzed data; M.N. wrote the manuscript with contributions from T.M. and M.Y.

DECLARATION OF INTERESTS

M.Y. and M.N. had filed an international patent application on the development and use of SHG-specific dye (PCT/JP2014/063754). T.M. declares no competing interests.

Received: July 26, 2018
Revised: October 1, 2018
Accepted: November 1, 2018
Published: November 30, 2018

REFERENCES

Ben-Oren, I., Peleg, G., Lewis, A., Minke, B., and Loew, L. (1996). Infrared nonlinear optical measurements of membrane potential in photoreceptor cells. Biophys. J. *71*, 1616–1620.

Brown, E., McKee, T., diTomaso, E., Pluen, A., Seed, B., Boucher, Y., and Jain, R.K. (2003). Dynamic imaging of collagen and its modulation in tumors in vivo using second-harmonic generation. Nat. Med. *9*, 796–800.

Campagnola, P.J., Wei, M.D., Lewis, A., and Loew, L.M. (1999). High-resolution nonlinear optical imaging of live cells by second harmonic generation. Biophys. J. *77*, 3341–3349.

Celik, E., Faridi, M.H., Kumar, V., Deep, S., Moy, V.T., and Gupta, V. (2013). Agonist leukadherin-1 increases CD11b/CD18-dependent adhesion via membrane tethers. Biophys. J. *105*, 2517–2527.

D'Souza-Schorey, C., van Donselaar, E., Hsu, V.W., Yang, C., Stahl, P.D., and Peters, P.J. (1998). ARF6 targets recycling vesicles to the plasma membrane: insights from an ultrastructural investigation. J. Cell Biol. *140*, 603–616.

Grecco, H.E., Schmick, M., and Bastiaens, P.I. (2011). Signaling from the living plasma membrane. Cell *144*, 897–909.

Mattheyses, A.L., Simon, S.M., and Rappoport, J.Z. (2010). Imaging with total internal reflection fluorescence microscopy for the cell biologist. J. Cell Sci. *123*, 3621–3628.

Moen, E.K., Ibey, B.L., and Beier, H.T. (2014). Detecting subtle plasma membrane perturbation in living cells using second harmonic generation imaging. Biophys. J. *106*, L37–L40.

Nuriya, M., Fukushima, S., Momotake, A., Shinotsuka, T., Yasui, M., and Arai, T. (2016). Multimodal two-photon imaging using a second harmonic generation-specific dye. Nat. Commun. *7*, 11557.

Nuriya, M., Jiang, J., Nemet, B., Eisenthal, K.B., and Yuste, R. (2006). Imaging membrane potential in dendritic spines. Proc. Natl. Acad. Sci. U S A *103*, 786–790.

Nuriya, M., and Yasui, M. (2010). Membrane potential dynamics of axons in cultured hippocampal neurons probed by second-harmonic-generation imaging. J. Biomed. Opt. *15*, 020503.

Pavone, F.S., and Campagnola, P.J. (2013). Second Harmonic Generation Imaging, First Edition (Taylor & Francis).

Quader, S., Cabral, H., Mochida, Y., Ishii, T., Liu, X., Toh, K., Kinoh, H., Miura, Y., Nishiyama, N., and Kataoka, K. (2014). Selective intracellular delivery of proteasome inhibitors through pH-sensitive polymeric micelles directed to efficient antitumor therapy. J. Control. Release *188*, 67–77.

Rama, S., Vetrivel, L., and Semyanov, A. (2010). Second-harmonic generation voltage imaging at subcellular resolution in rat hippocampal slices. J. Biophotonics *3*, 784–790.

Reeve, J.E., Anderson, H.L., and Clays, K. (2010). Dyes for biological second harmonic generation imaging. Phys. Chem. Chem. Phys. *12*, 13484–13498.

Resh, M.D. (1999). Fatty acylation of proteins: new insights into membrane targeting of myristoylated and palmitoylated proteins. Biochim. Biophys. Acta *1451*, 1–16.

Sacconi, L., Dombeck, D.A., and Webb, W.W. (2006). Overcoming photodamage in second-harmonic generation microscopy: real-time optical recording of neuronal action potentials. Proc. Natl. Acad. Sci. U S A *103*, 3124–3129.

Shim, S.H., Xia, C., Zhong, G., Babcock, H.P., Vaughan, J.C., Huang, B., Wang, X., Xu, C., Bi, G.Q., and Zhuang, X. (2012). Super-resolution fluorescence imaging of organelles in live cells with photoswitchable membrane probes. Proc. Natl. Acad. Sci. U S A *109*, 13978–13983.

Steyer, J.A., and Almers, W. (2001). A real-time view of life within 100 nm of the plasma membrane. Nat. Rev. Mol. Cell Biol. *2*, 268–275.

Zacharias, D.A., Violin, J.D., Newton, A.C., and Tsien, R.Y. (2002). Partitioning of lipid-modified monomeric GFPs into membrane microdomains of live cells. Science *296*, 913–916.

ISCI, Volume *9*

Supplemental Information

High-Resolution Plasma Membrane-Selective Imaging by Second Harmonic Generation

Takaha Mizuguchi, Masato Yasui, and Mutsuo Nuriya

Transparent Methods

CHO (Chinese Hamster Ovary) cell culture

CHO cells were maintained and used for analyses as described previously (Nuriya et al., 2016). Briefly, CHO cells that were originally obtained from the ATCC (Manassas, VA, USA) were maintained in culture media (10% fetal bovine serum in Dulbecco's modified Eagle's medium supplemented with penicillin and streptomycin) in a humidified 5% CO_2 incubator at 37°C until use. For imaging, CHO cells were plated on poly-L-lysine-coated coverslips (ϕ12 mm, 0.19 – 0.25 mm in thickness; Asahi Techno Glass, Yoshida, Shizuoka, Japan) in 35-mm culture dishes at a density of 0.5–2 × 10^4 cells/35-mm dish.

Transduction of CHO cells

CHO cells were transduced with actin-GFP, tubulin-GFP, or plasma membrane-attached GFP (GFP fused to the myristoylation/palmitoylation sequence of Lck tyrosine kinase) using the baculovirus-based BacMam CellLight Gene Delivery System (Thermo Fisher Scientific, Waltham, MA, USA), according to the manufacturer's instructions. Briefly, CHO cells on coverslips were transferred to a 4-well plate with 400 μL of original growth medium and incubated for 2–3 days with CellLight reagent with non-replicable baculovirus-containing genes encoding GFP-fused

proteins. Gene expression was examined by epi-fluorescence microscopy (Olympus CK53; Shinjuku, Tokyo, Japan) before use. To visualize endocytosed vesicles, CHO cells were incubated with 500 μg/mL 10-kDa-dextran-conjugated Alexa Fluor 594 (Thermo Fisher Scientific) for 30 min at 37°C before imaging.

Multimodal two-photon imaging

The MaitaiHP (Newport, Irvine, CA, USA) femtosecond laser was tuned to 950 nm and imaging was performed using the FV1000MPE microscope system (Olympus) with a 60× objective lens (N.A. 0.9, W.D. 2 mm). The laser power immediately after the objective lens was <20 mW. Cells grown on poly-L-lysine-coated coverslips were transferred to an imaging chamber, filled with 20–50 μM Ap3 (Funakoshi, Bunkyo, Tokyo, Japan) in imaging buffer containing 125 mM NaCl, 5 mM KCl, 10 mM dextrose, 10 mM HEPES, 1 mM $MgCl_2$, 2 mM $CaCl_2$, pH 7.3. As previously reported (Nuriya et al., 2016), cells emitted SHG signals immediately after staining with Ap3; even after recording for 3 h, signals remained stable with <20% loss of intensity, suggesting very little flip-flop movement or permeation of Ap3 dye at the plasma membrane. SHG signals were collected using a photomultiplier tube (PMT) with a narrow bandpass filter (465–485 nm). For simultaneous two-photon fluorescence imaging, fluorescence signals were simultaneously collected using

external PMTs after using 495–540 nm and 610–710 nm bandpass filters. To evaluate the spatial resolution of the system, TetraSpeck Fluorescent Microspheres of 100 nm diameters (Thermo Fisher Scientific) were used, with fluorescence detected at 610–710 nm.

Data Analyses

Imaging data were analyzed using ImageJ (National Institutes of Health, Bethesda, MD, USA) and MATLAB (MathWorks, Natick, MA, USA), and statistical analyses were performed using OriginPro (OriginLab, Northampton, MA, USA) and SPSS (IBM, Armonk, NY, USA). Images were processed using 1-pixel Gaussian blur filters. For analyses of the distances between the plasma membrane and cytoskeletons, all data for Ap3-SHG obtained from the plot profile across the plasma membrane were fit using a Gaussian equation. In the case of actin and tubulin, data obtained from regions outside of the cell to 50 nm beyond the point of the first peak inside the cell were used for Gaussian fitting. The distances were defined as the distances between the centers of the Gaussian fits of Ap3-SHG and GFP-TPF signals. Data are presented as means ± standard deviation and box plots show 25, 50, and 75 percentiles.

References

Nuriya, M., Fukushima, S., Momotake, A., Shinotsuka, T., Yasui, M., and Arai, T. (2016). Multimodal two-photon imaging using a second harmonic generation-specific dye. Nature communications *7*, 11557.